

See discussions, stats, and author profiles for this publication at: <https://www.researchgate.net/publication/232249405>

Synthesis and biological evaluation of new 5-benzylated 4-oxo-3,4-dihydro-5H-pyridazino[4,5-b]indoles as PI3K α inhibitors

ARTICLE in EUROPEAN JOURNAL OF MEDICINAL CHEMISTRY · SEPTEMBER 2012

Impact Factor: 3.45 · DOI: 10.1016/j.ejmech.2012.09.001 · Source: PubMed

CITATIONS

6

READS

52

13 AUTHORS, INCLUDING:



Cédric Logé

University of Nantes

47 PUBLICATIONS 442 CITATIONS

SEE PROFILE



Jana Sopkova-de Oliveira Santos

Université de Caen Normandie

128 PUBLICATIONS 1,585 CITATIONS

SEE PROFILE



Laurent Meijer

ManRos Therapeutics

411 PUBLICATIONS 20,688 CITATIONS

SEE PROFILE



Sandrine Ruchaud

French National Centre for Scientific Resea...

51 PUBLICATIONS 2,161 CITATIONS

SEE PROFILE



Original article

Synthesis and biological evaluation of new 5-benzylated 4-oxo-3,4-dihydro-5H-pyridazino[4,5-*b*]indoles as PI3K α inhibitors

Amélie Bruel^{a,*}, Cédric Logé^{a,*}, Marie-Ludivine de Tauzia^b, Myriam Ravache^c, Rémy Le Guevel^c, Christiane Guillouzo^c, Jean-François Lohier^d, Jana Sopkova-de Oliveira Santos^e, Olivier Lozach^f, Laurent Meijer^f, Sandrine Ruchaud^f, Hélène Bénédicti^b, Jean-Michel Robert^a

^a Université de Nantes, Nantes Atlantique Universités, Laboratoire de Chimie Thérapeutique, Cibles et Médicaments des Infections et du Cancer, IICIMED-EA 1155,

UFR Sciences Pharmaceutiques, 1 rue Gaston Veil, Nantes F-44035 Cedex 1, France

^b Centre de Biophysique Moléculaire, Centre National de la Recherche Scientifique (CNRS), UPR 4301, Université d'Orléans et INSERM, rue Charles Sadron, 45071 Orléans Cedex 2, France

^c Plate-forme ImpACcell, UMS-3480, Université de Rennes 1, Campus de Villejean, 2 avenue du Professeur Léon Bernard, 35043 Rennes Cedex, France

^d Laboratoire de Chimie Moléculaire et Thioorganique (LCMT), UMR CNRS 6507, INC3M, FR 3038, Labex EMC3, ENSICAEN & Université de Caen, 14050 Caen, France

^e Centre d'Etude et de Recherche sur le Médicament de Normandie (CERMN), UPRES EA 4258, FR CNRS 3038, INC3M, UFR des Sciences Pharmaceutiques, Université de Caen Basse-Normandie, Boulevard Becquerel, 14032 Caen Cedex, France

^f CNRS-USR3151, Protein Phosphorylation & Human Disease, Station Biologique, B.P.74, F-29682 Roscoff Cedex, France

ARTICLE INFO

Article history:

Received 9 July 2012

Received in revised form

30 August 2012

Accepted 1 September 2012

Available online 10 September 2012

Keywords:

4-oxo-3,4-dihydro-5H-pyridazino[4,5-*b*]indoles

Phosphoinositide 3-kinase (PI3K)

Dual-specificity tyrosine phosphorylation-regulated kinase 1A (DYRK1A)

Kinase inhibitors

Anti-proliferative effects

ABSTRACT

A series of novel 5-benzylated 4-oxo-3,4-dihydro-5H-pyridazino[4,5-*b*]indoles was synthesized through a newly developed approach. All these compounds were evaluated against DYRK1A, CDK5 and PI3K α and showed promising inhibitory activities against PI3K α with most IC₅₀ values in the micromolar range. Among them, compound **18** was strongly considered as the most interesting compound with an IC₅₀ value of 0.091 μ M. This series exhibited also significant anti-proliferative effects in various human cancer cell lines including those resulting in activation of the PI3K pathway.

© 2012 Elsevier Masson SAS. All rights reserved.

1. Introduction

During the past few years, the pyridazino[4,5-*b*]indole scaffold (Fig. 1a), an “aza-carboline”, has found considerable pharmaceutical interest, and a large number of derivatives have shown a wide range of biological activities [1]. The natural β -carboline harmine itself (Fig. 1b), was recently shown to inhibit dual-specificity tyrosine phosphorylation-regulated kinase 1A (DYRK1A) activity, a kinase implicated in neurodegenerative diseases as Down syndrome and Alzheimer disease, by interacting with residues Leu241 (hinge region) and Lys188 in the ATP-binding pocket via two hydrogen bonds to the methoxy group and the nitrogen atom

of the pyridinyl ring, respectively (PDB code: 3ANR) [2,3]. Due to the biological importance of these compounds, we aimed to investigate new representatives of this tricyclic ring system based on a 4-oxo-3,4-dihydro-5H-pyridazino[4,5-*b*]indole scaffold able to modulate a kinase activity through a competitive inhibition at the ATP binding site (Fig. 1c). These indole-fused pyridazinones could contain the molecular features required for a high affinity [4]: key hydrogen bonds which could interact with the so-called hinge part present in each kinase but especially various substituted benzyl peripheral groups attached to the N-5 position of this privileged structure which could target a pocket not addressed by ATP to gain binding affinity and selectivity. On the basis of this strategy, twenty-one compounds were synthesized and evaluated both in selected kinase assays (the dual-specificity kinase DYRK1A, the serine/threonine kinase CDK5 and the phosphoinositide 3-kinases (PI3Ks), which are therapeutic targets in neurodegenerative

* Corresponding author. Tel.: +33 (0)2 40 41 11 08; fax: +33 (0)2 40 41 28 76.
E-mail address: cedric.loge@univ-nantes.fr (C. Logé).

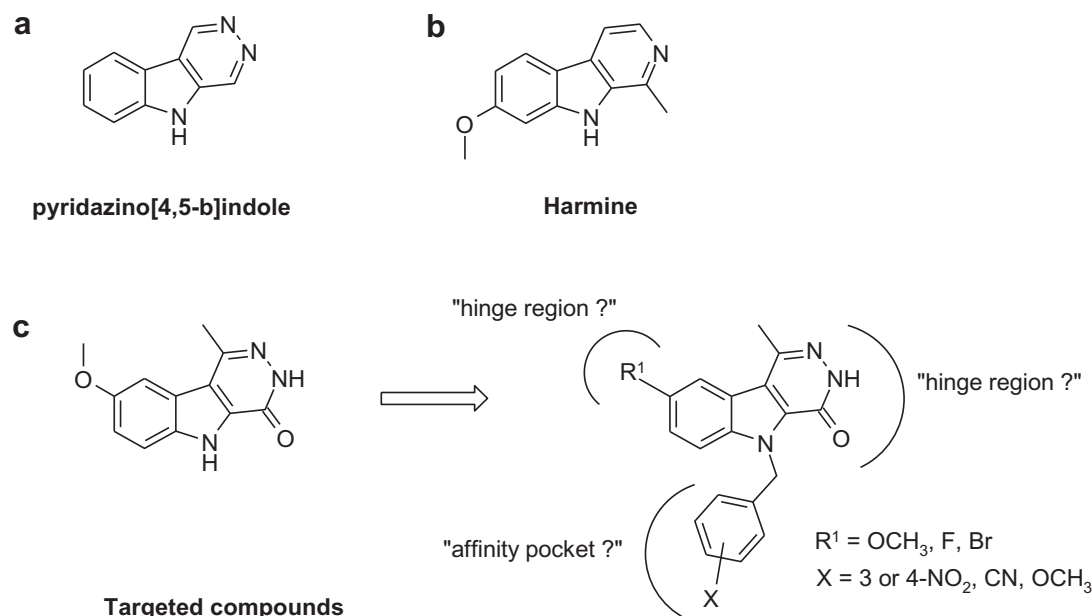


Fig. 1. Structures of pyridazino[4,5-*b*]indole (a), harmine (b) and the design concept of 5-benzylated-4-oxo-3,4-dihydro-5H-pyridazino[4,5-*b*]indole.

diseases or cancer) and for their in vitro anti-proliferative potencies against six human cancer cell lines. As these compounds were made accessible by short and convenient synthetic pathways, they could constitute ideal starting points for hit discovery.

2. Chemistry

5-substituted 4-oxo-3,4-dihydro-5H-pyridazino[4,5-*b*]indoles are generally prepared by introduction of the desired alkyl residue at the indole nitrogen before the formation of the pyridazinone unit, using 2-alkoxycarbonyl-3-acylindole as the substrate [5,6]. Interestingly, Haider et al. have shown that 5-alkyl-4-methyl-2,5-dihydro-1H-pyridazino[4,5-*b*]indole-1-ones can be prepared by selective monoalkylation of N-5 in the parent compound with stoichiometric amounts of alkylating agents [7]. Taking into account these two main observations, we decided to apply a similar strategy for the condensed pyridazino[4,5-*b*]indole-4-one scaffold.

The synthetic route to obtain the 5-benzylated compounds is shown in Scheme 1. Key intermediates ethyl indole-2-carboxylates (**4**, **7**, **8**) can be prepared by intra-molecular cyclization of the corresponding ethyl pyruvate 4-bromophenylhydrazones (**3**) in polyphosphoric acid (PPA) as a catalyst, according to Fischer's indole synthesis or by esterification of commercially 5-fluoro (**5**) and 5-methoxyindol-2-carboxylic acids (**6**). Friedel–Crafts acylation using aluminium trichloride and acetyl chloride gave indoles **9** and **10** with good yields. Moderate yield obtained for compounds **11** was due to the effect of the electron-donating methoxy group which activates the benzene ring and orients electrophilic attacks in ortho position. Condensation of hydrazine provided 4-oxo-3,4-dihydro-5H-pyridazino[4,5-*b*]indoles (**12**–**14**). Finally, and as expected, treatment of these compounds with sodium hydride and 3- or 4-substituted benzyl bromides afforded the target molecules **15**–**32**. The structure of **25** was confirmed by a single-crystal X-ray diffraction (Fig. 2).

3. Results and discussion

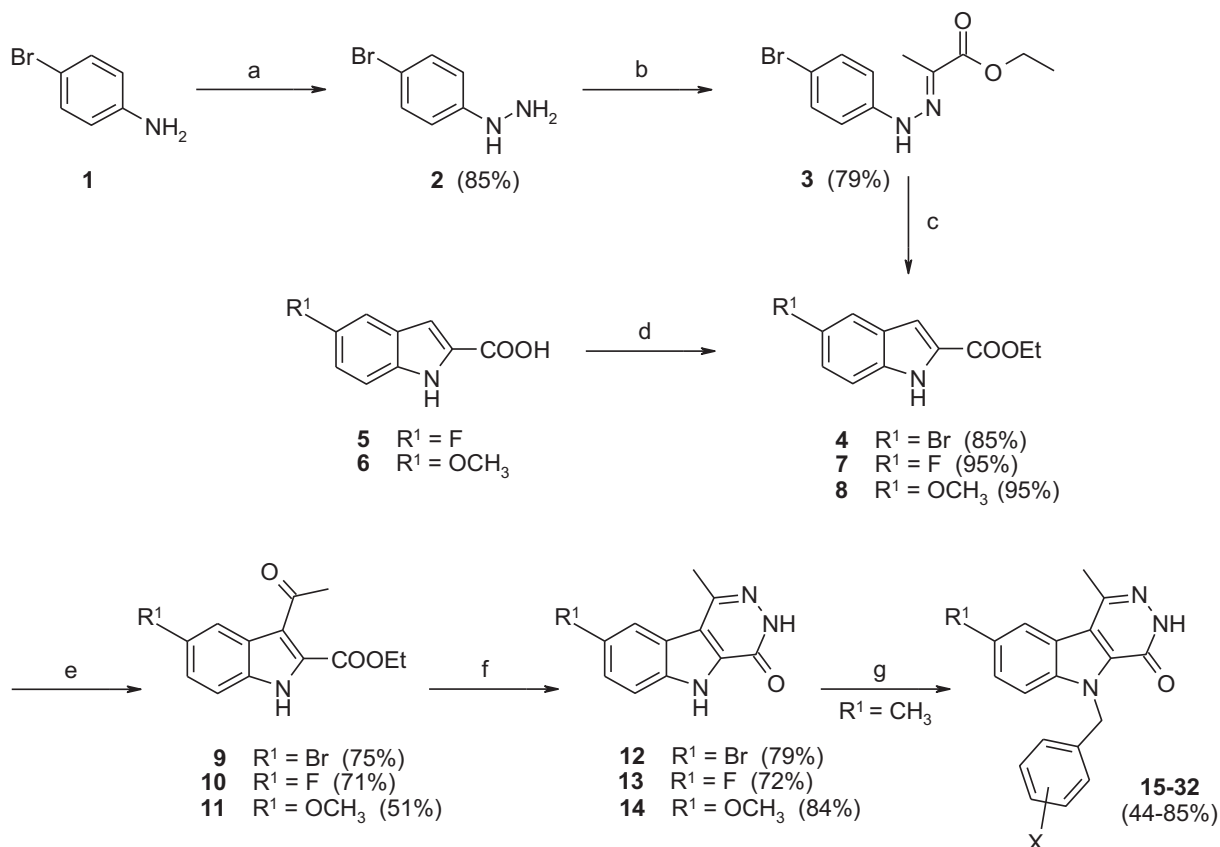
3.1. Kinase assays

Twenty-one compounds were tested against three representative kinases: DYRK1A, CDK5/p25 and PI3K p110 isoforms (α and γ).

The results are summarized in Table 1. All the 5-benzylated series (**15**–**32**) were considered inactive on both DYRK1A and CDK5/p25 since they displayed IC₅₀ values above 10 μ M, while they showed promising inhibitory activities against PI3K α with most IC₅₀ values in the micromolar range. The 8-brominated molecule **18** bearing a cyano substituent at the meta position of the benzyl group was strongly considered as the most interesting compound with an IC₅₀ value of 0.091 μ M, only 10-fold upper than that of PI-103, the well-known dual isoform-selective class I PI3K and mammalian target of rapamycin (mTOR) inhibitor used as the positive control [8]. This compound also showed sub-micromolar activity on the p110 gamma isoform of PI3K. These results are not surprising since tyrosine and serine/threonine kinases are closely related to each other but only distantly related to the PI3K family [9,10]. Therefore, as the three-dimensional space in the ATP-binding pocket of PI3K is larger than the corresponding spaces found in other protein kinases [11,12], our sterically encumbered 5-benzylated compounds should preferentially inhibit the lipid kinase family. Interestingly, unsubstituted analogues at position 5 (**13** and **14**) have led to compounds with micromolar activity on DYRK1A, suggesting that small flat structures can also be accommodated in the ATP binding site of this kinase.

3.2. Molecular modeling

To examine possible binding mode for compound **18** inside the ATP-binding site of PI3K, we have carried out molecular modeling studies into the existing crystal structure of p110 gamma isoform in complex with a known inhibitor at 2.40 Å resolution (PDB code, 1E7V) (PDB code: 1E7V) [12] since the co-crystal structure of p110 alpha isoform with a small ligand inhibitor has not been resolved yet. The docking result indicated that the pyridazinone ring could form two hydrogen bonding interactions with key PI3K hinge region residue Val882 (Fig. 3) while the electron-withdrawing cyano substituent in the meta position of the benzyl ring could interact with the hydroxyl side chain of Ser806, a residue that is conserved in all PI3Ks (equivalent to Ser774 in PI3K α) [13]. The heavier bromine atom is oriented toward a deeper affinity pocket defined among other by Lys833, Asp841, Ile879 and Asp964, which is located at the back of the ATP site and was shown to be crucial in



Scheme 1. Reagents and conditions: (a) (i) NaNO_2 , HCl , 0°C , 15 min; (ii) SnCl_2 , HCl , 0°C , 4 h; (b) ethyl pyruvate, EtOH , reflux, 5 h; (c) PPA, 85°C , 3 h; (d) SOCl_2 , EtOH , reflux, 3 h; (e) AlCl_3 , CH_3COCl , CH_2Cl_2 , reflux, 3 h or r.t. 5 h; (f) hydrazine hydrate, EtOH , reflux, 5 h; (g) (i) NaH , DMF , r.t., 30 min; (ii) benzyl bromides, DMF , r.t., 8 h.

controlling inhibitor potency [14,15] and could form an additional halogen bond interaction with the carboxylate side chain of Asp841 ($d = 3.085 \text{ \AA}$).

3.3. Cell effects

Six human cancer cell lines (hepatocellular carcinoma Huh-7, colorectal adenocarcinoma Caco2, colorectal carcinoma HCT-116, breast carcinoma MDA-MB-231, prostate carcinoma PC3 and lung carcinoid NCI-H727) and one normal cell line (fibroblasts) were used in our experiments. The results are presented in Table 2.

All the compounds were found to be as active as PI-103 in all tumor cell lines showing significant antitumor activity with IC_{50} values ranging from $0.4 \mu\text{M}$ for PC3 to $15 \mu\text{M}$ for HCT-116, but it clearly appeared that most compounds bearing a fluorine atom at position C-8 (**21**, **22** and **26**) were the most interesting as they did not inhibit the growth of normal fibroblasts and they exhibited the best antitumor activities in the PC3 and MDA-MB-231 cell lines with an IC_{50} value lower than $1 \mu\text{M}$.

However, when compared compound **18** which was a potent $\text{PI3K}\alpha$ inhibitor ($\text{IC}_{50} = 91 \text{ nM}$, Table 1) and compounds **21**, **22** and **26** which were considered inactive on this enzyme ($\text{IC}_{50} > 10 \mu\text{M}$),

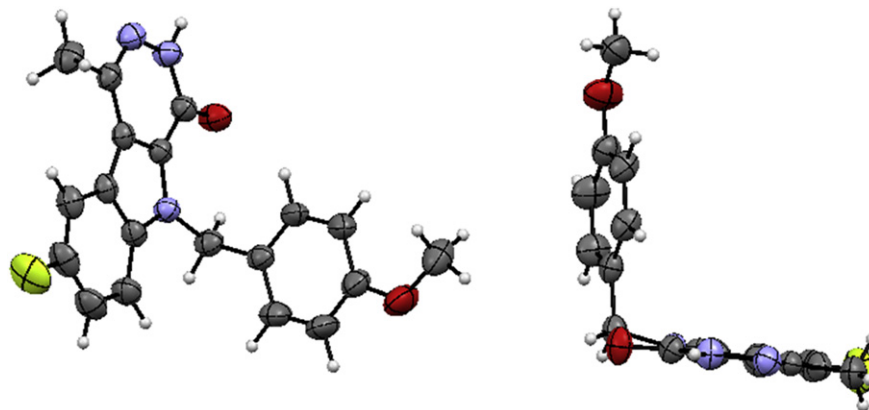
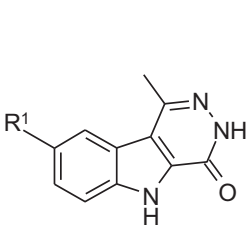
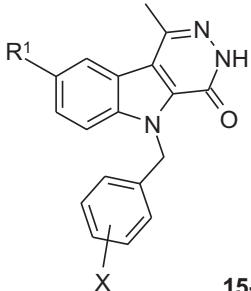


Fig. 2. ORTEP diagram of compound **25**.

Table 1

Kinase inhibition (IC₅₀ values in μM ; NT = not tested ; values lower than 10 μM are highlighted in bold).

						
12-14		15-32				
Cpds	R ¹	X	DYRK1A	CDK5/p25	PI3K α	PI3K γ
12	Br		NT	NT	NT	NT
13	F		5.6	>10	>10	NT
14	OMe		5	>10	>10	NT
15	Br	4-NO ₂	>10	>10	6	>10
16	Br	3-NO ₂	>10	>10	5.1	4.1
17	Br	4-CN	>10	>10	1.9	>10
18	Br	3-CN	>10	>10	0.091	0.295
19	Br	4-OMe	>10	>10	1.5	5.2
20	Br	3-OMe	>10	>10	1.5	2.2
21	F	4-NO ₂	>10	>10	>10	NT
22	F	3-NO ₂	>10	>10	>10	NT
23	F	4-CN	>10	>10	>10	NT
24	F	3-CN	>10	>10	5.0	NT
25	F	4-OMe	>10	>10	4.2	NT
26	F	3-OMe	>10	>10	>10	NT
27	OMe	4-NO ₂	>10	>10	2.6	NT
28	OMe	3-NO ₂	>10	>10	1.8	NT
29	OMe	4-CN	>10	>10	2.9	NT
30	OMe	3-CN	>10	>10	3.3	NT
31	OMe	4-OMe	>10	>10	>10	NT
32	OMe	3-OMe	>10	>10	6.3	NT
PI-103			NT	NT	0.008	0.15
Roscovitine			11	0.2	NT	NT

we can be surprised to observe that these last three molecules showed the best antitumor activities in the prostate PC3 carcinoma cell line which has a well-known genetic abnormality resulting in activation of the PI3K pathway (e.g. deletion of the tumor

Table 2

Anti-proliferative activity in various cell types (IC₅₀ values in μM ; NT = not tested; the number in brackets indicate the percentage of cell diminution).

Cpds	Huh7	Caco2	MDA-MB-231	HCT 116	PC3	NCI-H727	Fibroblasts
12	1.5	2	6	5	3	3	8
13	1.5	4	4	5	3	2	10
14	3	8	5	15	7	5	20
15	1	2	4	2	1.5	1	2
16	2	3	5	4	5	4	5
17	2	2	4	2	2	3	2
18	2	2	4	5	2.5	4	4
19	1.5	2	5	4	2.5	5	4
20	2	2	4	2	2	5	3
21	5	2	2	5	0.6	5	>25
22	3	2	0.8	4	0.7	6	>25
23	3	2	1.5	5	1	4	>25
24	3	2	12	6	4	6	8
25	1	2	2	2	2.5	3	5
26	1.5	2	0.9	4	0.4	2	>25
27	3	5	2	5	3	2.5	4
28	1.5	5	4	4	2.5	4	2 (50%)
29	2	6	2	4	2 (50%)	2	5
30	2	3	3	5	2	4	5
31	NT	NT	NT	NT	NT	NT	NT
32	1	2	3	2	2.5	3	1
PI-103	1.5 (40%)	0.9	15	1	1.5	3 (30%)	1.5 (30%)
Roscovitine	12	5	12	7	10	20	>25

suppressor PTEN (phosphatase with tensin homology)) [16]; the same observation applies to colorectal HCT-116 carcinoma cell with a mutation in the p110 α kinase domain [16]. Such results may suggest that the anti-proliferative effects do not seem to be correlated with an inhibition of the PI3K p110 α isoform alone and that other mechanisms could be involved.

4. Conclusion

In summary, we reported the original synthesis and preliminary biological evaluation of new 5-benzylated 4-oxo-3,4-dihydro-5H-pyridazino[4,5-*b*]indoles with promising in vitro inhibitory activities against PI3K α and significant anti-proliferative effects in various cell types. However, even if the structure–activity relationships can be explained among the three proposed enzymes, the correlation between the PI3K α inhibitory activities and some observed cell effects is not obvious. Further investigations including downstream mediators of the PI3K pathway (Akt and mTOR kinases), cell cycle progression and induction of apoptosis should be done to refine the exact mechanism of these antitumoral agents.

5. Experimental

5.1. Chemistry

Melting points were determined using an Electrothermal IA9300 digital melting point apparatus and reported uncorrected. ¹H and ¹³C NMR spectra were recorded on a Bruker AC250 (250 MHz) or on Bruker Avance 400 spectrometer (400 MHz). Chemical shifts are expressed as δ values (ppm) relative to tetramethylsilane as internal standard (in NMR description, s = singlet, d = doublet, t = triplet, q = quadruplet, sext = sextuplet, m = multiplet and b = broad). Coupling constants *J* are given in Hertz. IR spectra were obtained in KBr pellets using a Perkin–Elmer Paragon FTIR 1000 PC spectrometer. Only the most significant absorption bands have been reported. Electrospray mass spectrometric analysis was performed on a Waters Acquity UPLC System

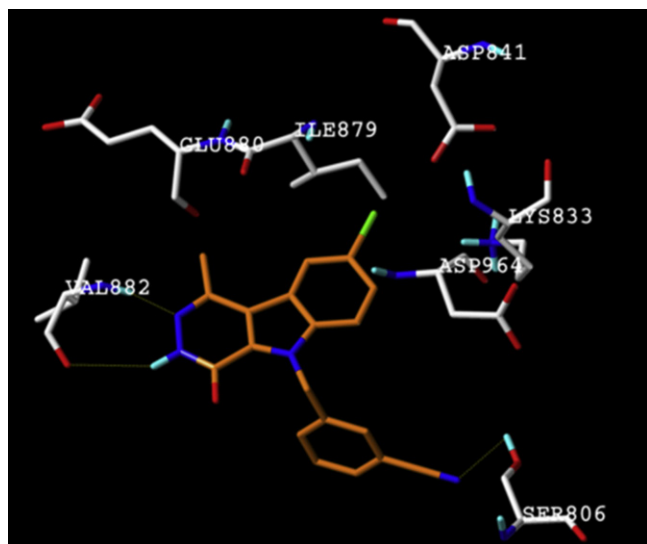


Fig. 3. Proposed binding mode for compound **18** into the ATP-binding site of PI3K γ (PDB code: 1E7V). The hydrogens bonds are indicated as yellow dotted lines. (For interpretation of the references to colour in this figure legend, the reader is referred to the web version of this article.)

ZQ 2000 single quadrupole. All reactions were monitored by thin-layer chromatography (TLC) using 0.2 mm-thick silica gel plates 60F-254 (5735 Merck). Column chromatography was carried out using silica gel 60 (70–230 Mesh, ASTM, Merck). Chemicals and solvents used were commercially available.

5.1.1. 4-Bromophenylhydrazine (**2**)

To an ice-cold aqueous solution of 12 N HCl (15 mL) was added 4-bromoaniline (4.00 g, 23.25 mmol) and dropwise an ice-cold solution of NaNO₂ (1.60 g, 23.19 mmol) in H₂O (5 mL). The reaction was stirred for 15 min at 0 °C. To the resulting mixture was added dropwise an ice-cold solution of tin(II) chloride (13.22 g, 69.73 mmol) in 12 N HCl (40 mL). The reaction mixture was stirred for 4 h at 0 °C. The precipitate was filtered, washed with 1 N HCl and poured into water where pH value was adjusted to 10 by adding 1 N NaOH. The crude product was extracted with Et₂O, dried over Na₂SO₄, filtered and concentrated under reduced pressure to give an orange solid. Yield 85%; ¹H NMR (400 MHz, DMSO-*d*₆) δ 7.25 (d, 2H, *J* = 8.8 Hz, Harom), 6.97 (s, 1H, NH), 6.76 (d, 2H, *J* = 8.8 Hz, Harom), 4.40 (s, 2H, NH₂).

5.1.2. Ethyl pyruvate 4-bromophenylhydrazone (**3**)

A mixture of 4-bromophenylhydrazine (**2**) (3.55 g, 18.98 mmol), ethyl pyruvate (2.65 g, 22.78 mmol) in EtOH (20 mL) was boiled under argon for 5 h. The cooled reaction mixture was then filtered and the precipitate was washed with water. The crude product was triturated with cyclohexane and filtered to give a yellow solid. Yield 79%; ¹H NMR (400 MHz, DMSO-*d*₆) δ 9.97 (s, 1H, NH), 7.48 (d, 2H, *J* = 8.8 Hz, Harom), 7.25 (d, 2H, *J* = 8.8 Hz, Harom), 4.23 (q, 2H, *J* = 7.2 Hz, CH₂), 2.09 (s, 3H, CH₃), 1.30 (t, 3H, *J* = 7.2 Hz, CH₃).

5.1.3. Ethyl 5-bromo-1H-indole-2-carboxylate (**4**)

A mixture of ethyl pyruvate 4-bromophenylhydrazone (**3**) (2.23 g, 7.82 mmol) and polyphosphoric acid (22 g) was heated to 85 °C for 3 h. The reaction mixture was then cooled, poured into ice-cold water and neutralized with saturated aqueous sodium bicarbonate. The crude product was extracted with EtOAc, dried over Na₂SO₄, filtered and concentrated under reduced pressure to give a pale yellow solid. Yield 85%; ¹H NMR (400 MHz, DMSO-*d*₆) δ 12.10 (s, 1H, NH), 7.87 (d, 1H, *J* = 0.8 Hz, Harom), 7.42 (dd, 1H, *J* = 8.8 and 0.8 Hz, Harom), 7.37 (dd, 1H, *J* = 8.8 and 1.2 Hz, Harom), 7.12 (d, 1H, *J* = 1.2 Hz, Harom), 4.34 (q, 2H, *J* = 7.2 Hz, CH₂), 1.34 (t, 3H, *J* = 7.2 Hz, CH₃).

5.1.4. General procedure for the synthesis of ethyl 1H-indole-2-carboxylates (**7**, **8**)

To a stirred solution of the appropriate acid (**5** or **6**) (11.16 mmol) in EtOH (60 mL) was added dropwise thionyl chloride (13.40 mmol) and the mixture was heated under reflux for 3 h. After cooling, water was added till a precipitate appeared. The crude product was filtered and dried over reduced pressure.

5.1.4.1. Ethyl 5-fluoro-1H-indole-2-carboxylate (7**).** Off-white solid. Yield 95%; ¹H NMR (400 MHz, DMSO-*d*₆) δ 11.99 (s, 1H, NH), 7.44 (dd, 1H, *J* = 9.2 and 4.8 Hz, Harom), 7.41 (dd, 1H, *J* = 9.8 and 2.8 Hz, Harom), 7.13 (ddd, 1H, *J* = 9.2; 9.2 and 2.8 Hz, Harom), 7.12 (d, 1H, *J* = 2.0 Hz, Harom), 4.33 (q, 2H, *J* = 7.2 Hz, CH₂), 1.33 (t, 3H, *J* = 7.2 Hz, CH₃).

5.1.4.2. Ethyl 5-methoxy-1H-indole-2-carboxylate (8**).** White solid. Yield 95%; ¹H NMR (400 MHz, DMSO-*d*₆) δ 11.77 (s, 1H, NH), 7.38 (dd, 1H, *J* = 8.8 and 0.8 Hz, Harom), 7.13 (d, 1H, *J* = 2.4 Hz, Harom), 7.08 (d, 1H, *J* = 0.8 Hz, Harom), 6.95 (dd, 1H, *J* = 8.8 and 2.4 Hz, Harom), 4.36 (q, 2H, *J* = 7.1 Hz, CH₂), 3.79 (s, 3H, OCH₃), 1.37 (t, 3H, *J* = 7.1 Hz, CH₃).

5.1.5. General procedure for the synthesis of ethyl 3-acetyl-1H-indole-2-carboxylates (**9**–**11**)

To a solution of the appropriate ester (**4**, **7** or **8**) (19.30 mmol) in freshly distilled CH₂Cl₂ (70 mL) was added aluminium chloride (38.60 mmol) and dropwise acetyl chloride (57.90 mmol). The mixture was boiled under argon (compounds **9** and **10**) for 3 h or was stirred at room temperature (compound **11**) for 5 h, then poured into ice-cold water and extracted with CH₂Cl₂. The organic layers were combined, dried over Na₂SO₄, filtered and concentrated under reduced pressure. The obtained residue was purified over silica gel chromatography eluting with CH₂Cl₂.

5.1.5.1. Ethyl 3-acetyl-5-bromo-1H-indole-2-carboxylate (9**).** White solid. Yield 75%; ¹H NMR (400 MHz, DMSO-*d*₆) δ 12.65 (s, 1H, NH), 8.12 (d, 1H, *J* = 1.6 Hz, Harom), 7.49 (d, 1H, *J* = 8.8 Hz, Harom), 7.46 (dd, 1H, *J* = 8.8 and 1.6 Hz, Harom), 4.43 (q, 2H, *J* = 7.2 Hz, CH₂), 2.60 (s, 3H, CH₃), 1.37 (t, 3H, *J* = 7.2 Hz, CH₃).

5.1.5.2. Ethyl 3-acetyl-5-fluoro-1H-indole-2-carboxylate (10**).** Off-white solid. Yield 71%; ¹H NMR (400 MHz, DMSO-*d*₆) δ 12.62 (s, 1H, NH), 7.71 (dd, 1H, *J* = 9.2 and 2.4 Hz, Harom), 7.57 (dd, 1H, *J* = 9.2 and 4.6 Hz, Harom), 7.25 (ddd, 1H, *J* = 9.2; 9.2 and 2.4 Hz, Harom), 4.45 (q, 2H, *J* = 7.2 Hz, CH₂), 2.63 (s, 3H, CH₃), 1.41 (t, 3H, *J* = 7.2 Hz, CH₃).

5.1.5.3. Ethyl 3-acetyl-5-methoxy-1H-indole-2-carboxylate (11**).** White solid. Yield 51%; ¹H NMR (400 MHz, DMSO-*d*₆) δ 12.38 (s, 1H, NH), 7.46 (d, 1H, *J* = 2.4 Hz, Harom), 7.45 (d, 1H, *J* = 8.8 Hz, Harom), 7.02 (dd, 1H, *J* = 8.8 and 2.4 Hz, Harom), 4.40 (q, 2H, *J* = 7.0 Hz, CH₂), 3.81 (s, 3H, CH₃), 2.62 (s, 3H, OCH₃), 1.40 (t, 3H, *J* = 7.0 Hz, CH₃).

5.1.6. General procedure for the synthesis of 4-oxo-3,4-dihydro-5H-pyridazino[4,5-*b*]indoles (**12**–**14**)

To a stirred solution of the appropriate ethyl 3-acetyl-1H-indole-2-carboxylates (**9**–**11**) (3.67 mmol) in EtOH (60 mL) was added dropwise hydrazine hydrate (7.34 mmol). The reaction was heated under reflux for 6 h, and stirred at room temperature for 16 h. After cooling, the resulting solution was concentrated under reduced pressure. The residue was washed with 1 N HCl, filtered and triturated with a small amount of diisopropyl ether.

5.1.6.1. 8-bromo-1-methyl-4-oxo-3,4-dihydro-5H-pyridazino[4,5-*b*]indole (12**).** Off-white solid. Yield 79%; mp >300 °C; IR (KBr, cm^{−1}) 3205 (NH), 1655 (CO), 790 (C–Br); ¹H NMR (400 MHz, DMSO-*d*₆) δ 13.01 (s, 1H, NH), 12.68 (s, 1H, NH), 8.23 (d, 1H, *J* = 1.6 Hz, Harom), 7.66 (dd, 1H, *J* = 8.8 and 1.6 Hz, Harom), 7.62 (d, 1H, *J* = 8.8 Hz, Harom), 2.72 (s, 3H, CH₃). ¹³C (100.6 MHz, DMSO-*d*₆) δ 155.33, 141.88, 137.71, 132.30, 129.49, 124.32, 123.15, 116.57, 115.24, 113.94, 20.10; MS (ESI) *m/z* (%): 278.0 [M + H]⁺; 280.0 [M + H+2]⁺ (Br isotope).

5.1.6.2. 8-fluoro-1-methyl-4-oxo-3,4-dihydro-5H-pyridazino[4,5-*b*]indole (13**).** Off-white solid. Yield 72%; mp >300 °C; IR (KBr, cm^{−1}) 3205 (NH), 1655 (CO); ¹H NMR (400 MHz, DMSO-*d*₆) δ 12.90 (s, 1H, NH), 12.63 (s, 1H, NH), 7.90 (dd, 1H, *J* = 9.3 and 2.4 Hz, Harom), 7.66 (dd, 1H, *J* = 9.2 and 4.8 Hz, Harom), 7.40 (ddd, 1H, *J* = 9.2; 9.2 and 2.4 Hz, Harom), 2.73 (s, 3H, CH₃). ¹³C (100.6 MHz, DMSO-*d*₆) δ 157.95 (*J* = 235.55 Hz), 155.44, 142.05, 135.70, 132.71, 121.66, 117.27, 115.44, 114.57, 107.10, 19.92; MS (ESI) *m/z* (%): 218.11 [M + H]⁺.

5.1.6.3. 8-methoxy-1-methyl-4-oxo-3,4-dihydro-5H-pyridazino[4,5-*b*]indole (14**).** Off-white solid. Yield 84%; mp >300 °C; IR (KBr, cm^{−1}) 3277 (NH), 1643 (CO), 1219, 1047 (C–O–C); ¹H NMR

(400 MHz, DMSO- d_6) δ 12.64 (s, 1H, NH), 12.52 (s, 1H, NH), 7.57 (d, 1H, J = 8.8 Hz, Harom), 7.52 (d, 1H, J = 2.4 Hz, Harom), 7.21 (dd, 1H, J = 8.8 and 2.4 Hz, Harom), 3.91 (s, 3H, OCH₃), 2.76 (s, 3H, CH₃). ¹³C (100.6 MHz, DMSO- d_6) δ 155.55, 154.92, 142.05, 134.09, 131.72, 121.93, 117.25, 117.01, 114.09, 103.37, 55.76, 20.19; MS (ESI) m/z (%): 230.14 [M + H]⁺.

5.1.7. General procedure for the synthesis of 5-benzyl-4-oxo-3,4-dihydro-5H-pyridazino[4,5-*b*]indoles (**15**–**32**)

To a solution of the appropriate 4-oxo-3,4-dihydro-5H-pyridazino[4,5-*b*]indoles (**12**–**14**) (0.92 mmol) in dry DMF (3 mL) was added sodium hydride (1.01 mmol, 60% w/w dispersion oil). The reaction mixture was stirred for 30 min at room temperature. The benzyl bromide (1.01 mmol) was slowly added dropwise. After being stirred at room temperature for 16 h, the solution was concentrated under reduced pressure. The resulting crude product was washed with water, filtered and triturated with EtOAc. The desired product was purified over silica gel chromatography eluting with CH₂Cl₂ to CH₂Cl₂/EtOH (98:2).

5.1.7.1. 8-bromo-1-methyl-5-(4-nitrobenzyl)-4-oxo-3,4-dihydro-5H-pyridazino[4,5-*b*]indole (15**).** Off-white solid. Yield 78%; mp >300 °C; IR (KBr, cm^{−1}): 3480 (NH), 1650 (CO), 1250, 1031 (C–O–C), 780 (C–Br); ¹H NMR (400 MHz, DMSO- d_6) δ 12.81 (s, 1H, NH), 8.32 (d, 1H, J = 1.8 Hz, Harom), 8.18 (d, 2H, J = 8.8 Hz, Harom), 7.78 (d, 1H, J = 9.0 Hz, Harom), 7.72 (dd, 1H, J = 9.0 and 1.8 Hz, Harom), 7.44 (d, 2H, J = 8.8 Hz, Harom), 6.29 (s, 2H, CH₂), 2.77 (s, 3H, CH₃). ¹³C (100.6 MHz, DMSO- d_6) δ 155.74, 147.01, 145.27, 142.08, 138.04, 130.25, 130.01, 128.13 (2C), 124.79, 124.03 (2C), 122.61, 117.00, 114.91, 113.89, 47.15, 20.21; MS (ESI) m/z (%): 413.0 [M + H]⁺; 415.0 [M + H + 2]⁺ (Br isotope).

5.1.7.2. 8-bromo-1-methyl-5-(3-nitrobenzyl)-4-oxo-3,4-dihydro-5H-pyridazino[4,5-*b*]indole (16**).** Off-white solid. Yield 44%; mp >300 °C; IR (KBr, cm^{−1}): 3232 (NH), 1656 (CO), 783 (C–Br); ¹H NMR (400 MHz, DMSO- d_6) δ 12.85 (s, 1H, NH), 8.32 (d, 1H, J = 1.8 Hz, Harom), 8.25 (s, 1H, Harom), 8.14 (d, 1H, J = 7.8 Hz, Harom), 7.89 (d, 1H, J = 8.8 Hz, Harom), 7.74 (dd, 1H, J = 8.8 and 1.8 Hz, Harom), 7.66 (d, 1H, J = 7.3 Hz, Harom), 7.62 (dd, 1H, J = 7.3 and 7.8 Hz, Harom), 6.27 (s, 2H, CH₂), 2.77 (s, 3H, CH₃). ¹³C (100.6 MHz, DMSO- d_6) δ 155.80, 148.08, 142.13, 139.82, 137.98, 133.85, 130.49, 130.15, 130.04, 124.80, 122.75, 122.60, 122.13, 117.03, 114.91, 113.95, 46.76, 20.20; MS (ESI) m/z (%): 413.0 [M + H]⁺; 415.0 [M + H + 2]⁺ (Br isotope).

5.1.7.3. 4-[(8-bromo-1-methyl-4-oxo-3,4-dihydro-5H-pyridazino[4,5-*b*]indolyl)methyl] benzonitrile (17**).** Off-white solid. Yield 52%; mp >300 °C; IR (KBr, cm^{−1}): 3449 (NH), 2224 (CN), 1659 (CO), 782 (C–Br); ¹H NMR (400 MHz, DMSO- d_6) δ 12.81 (s, 1H, NH), 8.32 (d, 1H, J = 1.8 Hz, Harom), 7.79 (d, 2H, J = 8.4 Hz, Harom), 7.77 (d, 1H, J = 8.8 Hz, Harom), 7.72 (dd, 1H, J = 8.8 and 1.8 Hz, Harom), 7.37 (d, 2H, J = 8.4 Hz, Harom), 6.23 (s, 2H, CH₂), 2.77 (s, 3H, CH₃). ¹³C (100.6 MHz, DMSO- d_6) δ 155.76, 143.27, 142.11, 138.06, 132.83 (2C), 130.26, 130.01, 127.89 (2C), 124.81, 122.61, 118.78, 116.99, 114.89, 113.93, 110.47, 47.22, 20.22; MS (ESI) m/z (%): 393.0 [M + H]⁺; 395.0 [M + H + 2]⁺ (Br isotope).

5.1.7.4. 3-[(8-bromo-1-methyl-4-oxo-3,4-dihydro-5H-pyridazino[4,5-*b*]indolyl)methyl] benzonitrile (18**).** Off-white solid. Yield 56%; mp >300 °C; IR (KBr, cm^{−1}): 3449 (NH), 2224 (CN), 1659 (CO), 782 (C–Br); ¹H NMR (400 MHz, DMSO- d_6) δ 12.81 (s, 1H, NH), 8.32 (d, 1H, J = 1.6 Hz, Harom), 7.89–7.80 (m, 2H, Harom), 7.79–7.70 (m, 2H, Harom), 7.58–7.50 (m, 2H, Harom), 6.19 (s, 2H, CH₂), 2.76 (s, 3H, CH₃). ¹³C (100.6 MHz, DMSO- d_6) δ 155.84, 142.14, 139.24, 137.98, 132.05, 131.61, 130.93, 130.24, 130.19, 130.00, 124.80, 122.66, 118.76, 117.03, 114.86, 113.96, 111.75, 46.79, 20.22; MS (ESI) m/z (%): 393.0 [M + H]⁺; 395.0 [M + H + 2]⁺ (Br isotope).

5.1.7.5. 8-bromo-5-(4-methoxybenzyl)-1-methyl-4-oxo-3,4-dihydro-5H-pyridazino[4,5-*b*]indole (19**).** Off-white solid. Yield 53%; mp >300 °C; IR (KBr, cm^{−1}): 3480 (NH), 1650 (CO), 1250, 1031 (C–O–C), 780 (C–Br); ¹H NMR (400 MHz, DMSO- d_6) δ 12.78 (s, 1H, NH), 8.25 (d, 1H, J = 1.6 Hz, Harom), 7.81 (d, 1H, J = 8.8 Hz, Harom), 7.69 (d, 1H, J = 8.8 Hz, Harom), 7.26 (d, 2H, J = 8.5 Hz, Harom), 6.86 (d, 2H, J = 8.5 Hz, Harom), 6.05 (s, 2H, CH₂), 3.70 (s, 3H, OCH₃), 2.73 (s, 3H, CH₃). ¹³C (100.6 MHz, DMSO- d_6) δ 158.81, 155.85, 142.07, 137.99, 130.16, 129.72, 129.57, 128.80 (2C), 124.67, 122.61, 116.74, 114.62, 114.29, 114.18 (2C), 55.22, 46.94, 20.22; MS (ESI) m/z (%): 398.0 [M + H]⁺; 400.0 [M + H + 2]⁺ (Br isotope).

5.1.7.6. 8-bromo-5-(3-methoxybenzyl)-1-methyl-4-oxo-3,4-dihydro-5H-pyridazino[4,5-*b*]indole (20**).** Off-white solid. Yield 70%; mp >300 °C; IR (KBr, cm^{−1}): 3451 (NH), 1654 (CO), 1266, 1042 (C–O–C), 779 (C–Br); ¹H NMR (400 MHz, DMSO- d_6) δ 12.78 (s, 1H, NH), 8.29 (d, 1H, J = 1.6 Hz, Harom), 7.79 (d, 1H, J = 8.8 Hz, Harom), 7.70 (dd, 1H, J = 8.8 and 1.6 Hz, Harom), 7.20 (dd, 1H, J = 8.1 and 7.8 Hz, Harom), 6.88 (s, 1H, Harom), 6.82 (dd, 1H, J = 8.2 and 2.1 Hz, Harom), 6.74 (d, 1H, J = 7.8 Hz, Harom), 6.09 (s, 2H, CH₂), 3.70 (s, 3H, OCH₃), 2.75 (s, 3H, CH₃). ¹³C (100.6 MHz, DMSO- d_6) δ 158.81, 155.85, 142.07, 137.99, 130.16, 129.72, 129.57, 128.80 (2C), 124.67, 122.61, 116.74, 114.62, 114.29, 114.18 (2C), 55.22, 46.94, 20.22; MS (ESI) m/z (%): 398.0 [M + H]⁺; 400.0 [M + H + 2]⁺ (Br isotope).

5.1.7.7. 8-fluoro-1-methyl-5-(4-nitrobenzyl)-4-oxo-3,4-dihydro-5H-pyridazino[4,5-*b*]indole (21**).** White solid. Yield 67%; mp >300 °C; IR (KBr, cm^{−1}): >3200 (NH), 1659 (CO), 1343 (NO₂); ¹H NMR (400 MHz, DMSO- d_6) δ 12.78 (s, 1H, NH), 8.19 (d, 2H, J = 8.8 Hz, Harom), 7.98 (dd, 1H, J = 9.6 and 2.4 Hz, Harom), 7.84 (dd, 1H, J = 9.2 and 4.4 Hz, Harom), 7.50 (ddd, 1H, J = 9.2; 9.2 and 2.4 Hz, Harom), 7.45 (d, 2H, J = 8.2 Hz, Harom), 6.29 (s, 2H, CH₂), 2.75 (s, 3H, CH₃). ¹³C (100.6 MHz, DMSO- d_6) δ 158.39 (J = 236.41 Hz), 155.86, 147.01, 145.42, 142.12, 135.95, 130.67, 128.17 (2C), 124.04 (2C), 121.28, 117.60, 115.96, 113.35, 107.78, 47.07, 20.09; MS (ESI) m/z (%): 353.04 [M + H]⁺.

5.1.7.8. 8-fluoro-1-methyl-5-(3-nitrobenzyl)-4-oxo-3,4-dihydro-5H-pyridazino[4,5-*b*]indole (22**).** Off-white solid. Yield 67%; mp >300 °C; IR (KBr, cm^{−1}): 3450 (NH), 1657 (CO), 1340 (NO₂); ¹H NMR (400 MHz, DMSO- d_6) δ 12.81 (s, 1H, NH), 8.27 (s, 1H, Harom), 8.14 (d, 1H, J = 7.6 Hz, Harom), 7.98–7.90 (m, 2H, Harom), 7.47–7.69 (m, 3H, Harom), 6.27 (s, 2H, CH₂), 2.74 (s, 3H, CH₃). ¹³C (100.6 MHz, DMSO- d_6) δ 155.92, 148.10, 142.17, 139.97, 135.91, 133.90, 130.57, 130.50, 122.76, 122.71, 121.33, 116.13, 115.86, 113.46, 46.78, 20.10 (2 carbones not visible); MS (ESI) m/z (%): 353.10 [M + H]⁺.

5.1.7.9. 4-[(8-fluoro-1-methyl-4-oxo-3,4-dihydro-5H-pyridazino[4,5-*b*]indolyl)methyl] benzonitrile (23**).** Off-white solid. Yield 65%; mp >300 °C; IR (KBr, cm^{−1}): >3200 (NH), 2229 (CN), 1659 (CO); ¹H NMR (400 MHz, DMSO- d_6) δ 12.77 (s, 1H, NH), 7.97 (dd, 1H, J = 9.4 and 4.1 Hz, Harom), 7.82 (dd, 1H, J = 9.1 and 4.3 Hz, Harom), 7.80 (d, 2H, J = 8.1 Hz, Harom), 7.48 (ddd, 1H, J = 9.1; 9.1 and 4.1 Hz, Harom), 7.39 (d, 2H, J = 8.1 Hz, Harom), 6.24 (s, 2H, CH₂), 2.76 (s, 3H, CH₃). ¹³C (100.6 MHz, DMSO- d_6) δ 158.19 (J = 238.46 Hz), 155.86, 143.38, 142.09, 135.93, 132.81 (2C), 130.65, 127.90 (2C), 121.28, 118.76, 117.60, 116.01, 113.25, 110.44, 107.78, 47.22, 20.08; MS (ESI) m/z (%): 333.13 [M + H]⁺.

5.1.7.10. 3-[(8-fluoro-1-methyl-4-oxo-3,4-dihydro-5H-pyridazino[4,5-*b*]indolyl)methyl] benzonitrile (24**).** Off-white solid. Yield 45%; mp >300 °C; IR (KBr, cm^{−1}): 3159 (NH), 2233 (CN), 1656 (CO); ¹H NMR (400 MHz, DMSO- d_6) δ 12.74 (s, 1H, NH), 7.97–7.78 (m, 3H, Harom), 7.71 (m, 1H, Harom), 7.55–7.40 (m, 3H, Harom), 6.14 (s, 2H, CH₂), 2.70 (s, 3H, CH₃). ¹³C (100.6 MHz, DMSO- d_6) δ 158.13 (J = 236.45), 155.71, 141.91, 139.14, 135.65, 131.87, 131.36, 130.75,

130.41, 129.96, 121.13, 118.54, 117.37, 115.82, 113.20, 111.51, 107.64, 46.58, 19.88; MS (ESI) m/z (%): 333.10 $[M + H]^+$.

5.1.7.11. 8-fluoro-5-(4-methoxybenzyl)-1-methyl-4-oxo-3,4-dihydro-5H-pyridazino[4,5-b]indole (25). Off-white solid. Yield 70%; mp >300 °C; IR (KBr, cm^{-1}) >3200 (NH), 1654 (CO), 1246, 1020 (C–O–C); ^1H NMR (400 MHz, DMSO- d_6) δ 12.74 (s, 1H, NH), 7.92 (dd, 1H, $J = 9.2$ and 2.4 Hz, Harom), 7.87 (dd, 1H, $J = 9.2$ and 4.4 Hz, Harom), 7.57 (ddd, 1H, $J = 9.2$; 9.2 and 2.4 Hz, Harom), 7.28 (d, 2H, $J = 8.6$ Hz, Harom), 6.86 (d, 2H, $J = 8.6$ Hz, Harom), 6.05 (s, 2H, CH_2), 3.70 (s, 3H, OCH_3), 2.73 (s, 3H, CH_3). ^{13}C (100.6 MHz, DMSO- d_6) δ 158.78, 158.22 ($J = 236.81$ Hz), 155.94, 142.05, 135.88, 130.53, 129.68, 128.84 (2C), 121.20, 117.20, 115.61, 114.15 (2C), 113.65, 107.50, 55.19, 46.93, 20.09; MS (ESI) m/z (%): 338.17 $[M + H]^+$.

5.1.7.12. 8-fluoro-5-(3-methoxybenzyl)-1-methyl-4-oxo-3,4-dihydro-5H-pyridazino[4,5-b]indole (26). Off-white solid. Yield 85%; mp >300 °C; IR (KBr, cm^{-1}) >3200 (NH), 1654 (CO), 1264, 1036 (C–O–C); ^1H NMR (400 MHz, DMSO- d_6) δ 12.75 (s, 1H, NH), 7.98–7.80 (m, 2H, Harom), 7.47 (m, 1H, Harom), 7.20 (m, 1H, Harom), 6.95–6.70 (m, 3H, Harom), 6.10 (s, 2H, CH_2), 3.70 (s, 3H, OCH_3), 2.74 (s, 3H, CH_3). ^{13}C (100.6 MHz, DMSO- d_6) δ 159.53, 158.25 ($J = 246.55$), 155.89, 142.07, 139.27, 136.01, 130.65, 129.94, 121.08, 119.22, 117.26, 115.50, 113.54, 113.43, 112.57, 107.35, 55.15, 47.40, 20.08; MS (ESI) m/z (%): 338.05 $[M + H]^+$.

5.1.7.13. 8-methoxy-1-methyl-5-(4-nitrobenzyl)-4-oxo-3,4-dihydro-5H-pyridazino[4,5-b]indole (27). Off-white solid. Yield 64%; mp = 288–289 °C; IR (KBr, cm^{-1}) >3200 (NH), 1659 (CO), 1342 (NO_2), 1215, 1035 (C–O–C); ^1H NMR (400 MHz, DMSO- d_6) δ 12.68 (s, 1H, NH), 8.18 (d, 2H, $J = 8.8$ Hz, Harom), 7.69 (d, 1H, $J = 9.0$ Hz, Harom), 7.57 (d, 1H, $J = 2.4$ Hz, Harom), 7.43 (d, 2H, $J = 8.8$ Hz, Harom), 7.24 (dd, 1H, $J = 9.0$ and 2.4 Hz, Harom), 6.27 (s, 2H, CH_2), 3.91 (s, 3H, OCH_3), 2.79 (s, 3H, CH_3). ^{13}C (100.6 MHz, DMSO- d_6) δ 155.97, 155.48, 146.96, 145.75, 142.22, 134.38, 129.69, 128.12 (2C), 124.03 (2C), 121.51, 117.58, 117.34, 112.73, 103.96, 55.83, 46.94, 20.31; MS (ESI) m/z (%): 365.13 $[M + H]^+$.

5.1.7.14. 8-methoxy-1-methyl-5-(3-nitrobenzyl)-4-oxo-3,4-dihydro-5H-pyridazino[4,5-b]indole (28). Off-white solid. Yield 64%; mp = 288–289 °C; IR (KBr, cm^{-1}) >3200 (NH), 1662 (CO), 1348 (NO_2), 1213, 1040 (C–O–C); ^1H NMR (400 MHz, DMSO- d_6) δ 12.70 (s, 1H, NH), 8.21 (s, 1H, Harom), 8.12 (d, 1H, $J = 7.2$ Hz, Harom), 7.79 (d, 1H, $J = 9.2$ Hz, Harom), 7.65 (d, 1H, $J = 7.6$ Hz, Harom), 7.63 (dd, 1H, $J = 7.6$ and 7.2 Hz, Harom), 7.56 (d, 1H, $J = 2.2$ Hz, Harom), 7.25 (dd, 1H, $J = 9.2$ and 2.2 Hz, Harom), 6.24 (s, 2H, CH_2), 3.90 (s, 3H, OCH_3), 2.77 (s, 3H, CH_3). ^{13}C (100.6 MHz, DMSO- d_6) δ 156.06, 155.53, 148.13, 142.38, 140.31, 134.38, 133.90, 130.50, 129.63, 122.72, 122.06, 121.55, 117.67, 117.42, 112.80, 101.01, 55.86, 46.71, 20.33; MS (ESI) m/z (%): 365.20 $[M + H]^+$.

5.1.7.15. 4-[(8-methoxy-1-methyl-4-oxo-3,4-dihydro-5H-pyridazino[4,5-b]indolyl)methyl] benzonitrile (29). Off-white solid. Yield 56%; mp >300 °C; IR (KBr, cm^{-1}) >3200 (NH), 2216 (CN), 1660 (CO), 1210, 1041 (C–O–C); ^1H NMR (400 MHz, DMSO- d_6) δ 12.68 (s, 1H, NH), 7.80 (d, 2H, $J = 8.4$ Hz, Harom), 7.69 (d, 1H, $J = 9.2$ Hz, Harom), 7.57 (d, 1H, $J = 2.4$ Hz, Harom), 7.36 (d, 2H, $J = 8.4$ Hz, Harom), 7.23 (dd, 1H, $J = 9.2$ and 2.4 Hz, Harom), 6.20 (s, 2H, CH_2), 3.90 (s, 3H, OCH_3), 2.78 (s, 3H, CH_3). ^{13}C (100.6 MHz, DMSO- d_6) δ 155.98, 155.47, 143.72, 142.24, 134.40, 132.80 (2C), 129.70, 127.89 (2C), 121.49, 118.83, 117.58, 117.32, 112.76, 110.36, 103.96, 55.83, 47.11, 20.31; MS (ESI) m/z (%): 345.10 $[M + H]^+$.

5.1.7.16. 3-[(8-methoxy-1-methyl-4-oxo-3,4-dihydro-5H-pyridazino[4,5-b]indolyl)methyl] benzonitrile (30). Off-white solid. Yield 52%;

mp >300 °C; IR (KBr, cm^{-1}) >3200 (NH), 2224 (CN), 1661 (CO), 1213, 1041 (C–O–C); ^1H NMR (400 MHz, DMSO- d_6) δ 12.68 (s, 1H, NH), 7.81 (s, 1H, Harom), 7.72–7.78 (m, 2H, Harom), 7.57 (d, 1H, $J = 2.2$ Hz, Harom), 7.55–7.49 (m, 2H, Harom), 7.24 (dd, 1H, $J = 9.2$ and 2.2 Hz, Harom), 6.15 (s, 2H, CH_2), 3.90 (s, 3H, OCH_3), 2.77 (s, 3H, CH_3). ^{13}C (100.6 MHz, DMSO- d_6) δ 156.04, 155.45, 142.26, 139.66, 134.32, 132.06, 131.51, 130.90, 130.17, 129.65, 121.53, 118.80, 117.56, 117.34, 112.79, 111.68, 103.99, 55.83, 46.66, 20.31; MS (ESI) m/z (%): 345.10 $[M + H]^+$.

5.1.7.17. 8-methoxy-5-(4-methoxybenzyl)-1-methyl-4-oxo-3,4-dihydro-5H-pyridazino[4,5-b]indole (31). Off-white solid. Yield 52%; mp = 247–248 °C; IR (KBr, cm^{-1}) >3200 (NH), 1652 (CO), 1245, 1030 (C–O–C); ^1H NMR (400 MHz, DMSO- d_6) δ 12.63 (s, 1H, NH), 7.75 (d, 1H, $J = 9.2$ Hz, Harom), 7.54 (d, 1H, $J = 2.4$ Hz, Harom), 7.25 (d, 2H, $J = 8.7$ Hz, Harom), 7.23 (dd, 1H, $J = 9.2$ and 2.4 Hz, Harom), 6.85 (d, 2H, $J = 8.7$ Hz, Harom), 6.02 (s, 2H, CH_2), 3.89 (s, 3H, OCH_3), 3.70 (s, 3H, OCH_3), 2.76 (s, 3H, CH_3). ^{13}C (100.6 MHz, DMSO- d_6) δ 158.71, 156.04, 155.26, 142.14, 134.38, 129.97, 129.57, 128.76 (2C), 121.45, 117.29, 117.02, 114.09 (2C), 113.09, 103.77, 55.79, 55.18, 46.79, 20.29; MS (ESI) m/z (%): 350.14 $[M + H]^+$.

5.1.7.18. 8-methoxy-5-(3-methoxybenzyl)-1-methyl-4-oxo-3,4-dihydro-5H-pyridazino[4,5-b]indole (32). Off-white solid. Yield 52%; mp = 247–248 °C; IR (KBr, cm^{-1}) >3200 (NH), 1655 (CO), 1267, 1038 (C–O–C); ^1H NMR (400 MHz, DMSO- d_6) δ 12.64 (s, 1H, NH), 7.70 (d, 1H, $J = 9.2$ Hz, Harom), 7.53 (d, 1H, $J = 2.2$ Hz, Harom), 7.23 (dd, 1H, $J = 9.2$ and 2.2 Hz, Harom), 7.19 (dd, 1H, $J = 8.0$ and 7.6 Hz, Harom), 6.86 (s, 1H, Harom), 6.81 (dd, 1H, $J = 8.0$ and 2.4 Hz, Harom), 6.74 (d, 1H, $J = 7.6$ Hz, Harom), 6.07 (s, 2H, CH_2), 3.90 (s, 3H, OCH_3), 3.70 (s, 3H, OCH_3), 2.77 (s, 3H, CH_3). ^{13}C (100.6 MHz, DMSO- d_6) δ 159.51, 156.02, 155.30, 142.17, 139.58, 134.48, 129.90, 129.67, 121.41, 119.20, 117.36, 117.06, 113.38, 112.99, 112.43, 103.76, 55.78, 55.12, 47.27, 20.29; MS (ESI) m/z (%): 350.14 $[M + H]^+$.

5.2. Biological evaluation

5.2.1. Kinase assays on CDK5/p25 and DYRK1A

Buffer A: 10 mM MgCl_2 , 1 mM EGTA, 1 mM DTT, 25 mM Tris–HCl (pH 7.5), 50 μg heparin/mL. Buffer C: 60 mM β -glycerophosphate, 15 mM p -nitrophenylphosphate, 25 mM Mops (pH 7.2), 5 mM EGTA, 15 mM MgCl_2 , 1 mM DTT, 1 mM sodium vanadate, 1 mM phenylphosphate. Kinase activities were assayed in Buffer A or C, at 30 °C, at a final ATP concentration of 15 μM . Blank values were subtracted and activities expressed in % of the maximal activity, i.e. in the absence of inhibitors. Controls were performed with appropriate dilutions of DMSO. CDK5/p25 (human, recombinant) was prepared as previously described [17]. Its kinase activity was assayed in buffer C, with 1 mg histone H1/mL, in the presence of 15 μM [γ -33P] ATP (3000 Ci/mmol; 10 mCi/mL) in a final volume of 30 μL . After 30 min incubation at 30 °C, 25 μL aliquots of supernatant were spotted onto 2.5 \times 3 cm pieces of Whatman P81 phosphocellulose paper, and 20 s later, the filters were washed five times (for at least 5 min each time) in a solution of 10 mL phosphoric acid/L of water. The wet filters were counted in the presence of 1 mL ACS (Amersham) scintillation fluid. DYRK1A (rat, recombinant, expressed in *Escherichia coli* as a GST fusion protein) was purified by affinity chromatography on glutathione-agarose and assayed as described for CDK5/p25 using myelin basic protein (1 mg/mL) as a substrate.

5.2.2. Kinase assays on PI3K (alpha and gamma)

The activity of the alpha isoform of PI3k was evaluated using a purified heterodimer (ref PV4788 from Invitrogen) composed of

the catalytic p110 α subunit (PIK3CA) and the regulatory p85 α subunit (PIK3R1). The activity of the gamma isoform was evaluated using the purified catalytic p110 γ subunit (PIK3CG) (ref PV4786 from Invitrogen). The ADAPTA™ kinase assay kit (Invitrogen) is a fluorescence-based immunoassay for the detection of ADP. It takes place in 384-well plates and can be divided into two phases: a kinase reaction phase, and an ADP detection phase. In the kinase reaction phase, the following components are mixed into the same well: 5 μ L of a solution containing 20 μ M ATP and 2 μ M PIP2 diluted in kinase assay buffer (50 mM HEPES pH 7.5, 100 mM NaCl, 0.03% CHAPS, 1 mM EGTA, 3 mM MgCl₂, 2 mM DTT), 2.5 μ L of kinase at the optimal concentration (222 ng/mL) diluted in kinase assay buffer, and 2.5 μ L of serial dilutions of inhibitors diluted in 4% DMSO and kinase assay buffer. For each inhibitor concentration, the assay was run in triplicate. The reaction was then incubated 60 min at room temperature. For the ADP detection phase, 5 μ L of a detection solution containing Europium-labeled anti-ADP antibody (6 nM), Alexa Fluor® 647 labeled ADP tracer (12 nM), and EDTA (30 mM, to stop the kinase reaction), diluted in TR-FRET dilution buffer (provided by the manufacturer) is added to the assay well. After 30 min of incubation at room temperature, the 384-well plates were read in a Victor V plate reader configured for HTRF (Perkin Elmer). Excitation was performed at 340 nm and emission was measured at 665 nm and 615 nm. The inhibition curve was then plotted as emission ratio 665 nm/615 nm versus inhibitor concentration. In order to calculate substrate conversion values (% conversion of ATP in ADP) from the raw TR–FRET emission ratios, an ATP–ADP titration curve was performed with a total nucleotide concentration of 10 μ M. The resulting TR–FRET emission ratio was plotted against the % conversion of ATP to ADP. The data of this curve were fit to a 3-parameter hyperbolic model with the following equation obtained from a GraphPad™ Prism® software:

$$Y = C + A \times (1 - (X/(B + X)))$$

The % conversion corresponding to each TR–FRET ratio was calculated using the following equation:

$$\% \text{ Conversion} = B \times \frac{(C + A - \text{Ratio})}{(\text{Ratio} - C)}$$

The % conversion was then plotted versus the concentration of inhibitor. The amount of inhibitor required to elicit a 50% change in the % conversion of ATP in ADP (the EC₅₀) was then determined. This EC₅₀ corresponds to the IC₅₀ value of the inhibitor.

5.2.3. Cell culture and survival assay

Skin diploid fibroblastic cells were provided by BIOPREDIC International Company (Rennes, France). Caco2 (REF ECACC: 86010202), Huh-7D12 (REF ECACC: 01042712), MDA-MB-231 (REF ECACC: 92020424), HCT-116 (REF ECACC: 91091005), PC3 (REF ECACC: 90112714) and NCI-H727 (REF ECACC: 94060303) cell lines were obtained from the ECACC collection. Cells were grown according to ECACC recommendations. The toxicity test of the compounds on these cells was as follows: 2×10^3 cells for HCT-116 cells or 4×10^3 for the other cells were seeded in 96 multiwell plates in triplicate and left for 24 h for attachment, spreading and growing. Then, cells were exposed for 48 h to increasing concentrations of the compounds, ranging from 0.1 to 25 μ M in a final volume of 120 μ L of culture medium. Cells were fixed in cooled 90% ethanol/5% acetic acid solution, nuclei were stained with Hoechst 3342 (Sigma) and counted using automated imaging analysis (Cellomics Arrayscan VTI/HCS Reader, Thermo/Scientific). The IC₅₀ were graphically determined.

5.3. Crystallographic analysis

Single crystals of compound **25** suitable for X-ray crystallographic analysis were obtained by slow diffusion from compound **25** solution (dichloromethane/diisopropyl ether). X-ray diffraction experiment was performed with graphite–monochromatized Mo K α radiation on a Bruker–Nonius Kappa CCD area detector diffractometer at 296 K. The data treatment was carried out with APEX II program [18]. The crystal structure was solved by direct methods using SHELXTL package [19] and refined by SHELX97 [20]. All non-hydrogen atoms were refined anisotropically and the hydrogen atoms were located from the electron density map and refined isotropically. Crystallographic data for compound **25** have been deposited at the Cambridge Crystallographic Data Centre, CCDC ID 889555. Copies of this information may be obtained free of charge from the Director, CCDC, 12 Union Road, Cambridge, CB2 1EZ, UK (+44-1223-336408; E-mail: deposit@ccdc.cam.ac.uk <http://www.ccdc.cam.ac.uk>).

5.4. Molecular modeling

Molecular modeling studies were performed using Sybyl software version 8.0 [21] running on a dell precision T3400 workstation. The three-dimensional structure of compound **18** was built from a standard fragments library, and its geometry was subsequently optimized using the Tripos force field [22] including the electrostatic term calculated from Gasteiger and Hückel atomic charges. Powell's method available in Maximin2 procedure was used for energy minimization until the gradient value was smaller than 0.001 kcal/mol Å. The structure of PI3K γ in complex with inhibitor LY294002 (PDB code, 1E7V) [12] was used as the template for docking. The original ligand as well as the water molecules were removed from the coordinates set. Flexible docking of molecule **18** into the ATP-binding site was performed using GOLD software [23]. The most stable docking model was selected according to the best scored conformation predicted by the GoldScore scoring function.

Acknowledgments

This work was supported by grant from the Canceropôle Grand Ouest.

Appendix A. Supplementary material

¹H and ¹³C NMR spectra for compounds **12**, **13**, **18** and **25** can be found, in the online version at <http://dx.doi.org/10.1016/j.ejmech.2012.09.001>.

References

- [1] (a) A. Monge, P. Parrado, M. Font, E. Fernández-Alvarez, Selective thromboxane synthetase and antihypertensive agents. New derivatives of 4-hydrazino-5H-pyridazino[4,5-b]indole, 4-hydrazinopyridazino[4,5-a]indole, and related compounds, *J. Med. Chem.* 30 (1987) 1029–1035; (b) A. Monge, I. Aldana, T. Alvarez, M. Font, E. Santiago, J.A. Latre, M.J. Bermejillo, M.J. Lopez-Unzu, New 5H-pyridazino[4,5-b]indole derivatives. Synthesis and studies as inhibitors of blood platelet aggregation and inotropics, *J. Med. Chem.* 34 (1991) 3023–3029; (c) M. Font, A. Monge, A. Cuartero, A. Elorriaga, J.J. Martínez-Irujo, E. Alberdi, E. Santiago, I. Prieto, J.J. Lasarte, P. Sarobe, F. Borrás, Indoles and pyridazino [4,5-b]indoles as nonnucleoside analog inhibitors of HIV-1 reverse transcriptase, *Eur. J. Med. Chem.* 30 (1995) 963–971; (d) A.A. El-Gendy, H.A. El-Banna, Synthesis and hypertensive activity of certain Mannich bases of 2-ethoxycarbonylindoles and 5H-pyridazino[4,5-b]indoles, *Arch. Pharm. Res.* 24 (2001) 21–26; (e) Y. Evanno, L. Dubois, M. Sevrin, F. Marguet, J. Froissant, R. Bartsch, C. Gille, 3-heteroaryl-3,5-dihydro-4-oxo-4H-pyridazino[4,5-b]indole-1-acetamide derivatives, their preparation and their application in therapy, *US 6,262,045 B1*. (f) N.C. Becknell, R.L. Hudkins, Fused [d]pyridazin-7-ones, *WO 2007/149557*.

- [2] Y. Ogawa, Y. Nonaka, T. Goto, E. Ohnishi, T. Hiramatsu, I. Kii, M. Yoshida, T. Ikura, H. Onogi, H. Shibuya, T. Hosoya, N. Ito, M. Hagiwara, Development of a novel selective inhibitor of the Down syndrome-related kinase Dyrk1A, *Nat. Commun.* 1 (2010) 1–9.
- [3] T. Adayev, J. Wegiel, Y.-W. Hwang, Harmine is an ATP-competitive inhibitor for dual-specificity tyrosine phosphorylation-regulated kinase 1A (Dyrk1A), *Arch. Biochem. Biophys.* 507 (2011) 212–218.
- [4] G. Keri, L. Orfi, D. Eros, B. Hegymegi-Barakonyi, C. Szantai-Kis, Z. Horvath, F. Waczek, J. Marosfalvi, I. Szabadkai, J. Pato, Z. Greff, D. Hafenbradl, H. Daub, G. Muller, B. Klebl, A. Ullrich, Signal transduction therapy with rationally designed kinase inhibitors, *Curr. Signal. Trans. Ther.* 1 (2006) 67–95.
- [5] A. Monge, I. Aldana, I. Lezamiz, E. Fernandez-Alvarez, A simple preparation of 4-oxo-3,4-dihydro-5H-pyridazino[4,5-b]indoles, *Synthesis-Stuttgart* 2 (1984) 160–161.
- [6] N. Haider, A. Wobus, Concise syntheses of 5-substituted pyridazino[4,5-b]indolones and diones, *ARKIVOC* vii (2008) 16–25.
- [7] H. El-Kashef, A.A.H. Farghaly, S. Floriani, N. Haider, Synthesis of 3-azaharman and other new azacarboline of the pyridazino[4,5-b]indole type, *ARKIVOC* xiv (2003) 198–209.
- [8] Q.W. Fan, Z.A. Knight, D.D. Goldenberg, W. Yu, K.E. Mostov, D. Stokoe, K.M. Shokat, W.A. Weiss, A dual PI3 kinase/mTOR inhibitor reveals emergent efficacy in glioma, *Cancer Cell* 9 (2006) 341–349.
- [9] E.D. Scheeff, P.E. Bourne, Structural evolution of the protein kinase-like superfamily, *PLoS Comput. Biol.* 1 (5) (2005) e49. 359–381.
- [10] B. Apse, J.A. Blair, B.Z. Gonzalez, T.M. Nazif, M.E. Feldman, B. Aizenstein, R. Hoffman, R.L. Williams, K.M. Shokat, Z.A. Knight, Targeted polypharmacology: discovery of dual inhibitors of tyrosine and phosphoinositide kinases, *Nat. Chem. Biol.* 4 (2008) 691–699.
- [11] S. Yaguchi, Y. Fukui, I. Koshimizu, H. Yoshimi, T. Matsuno, H. Gouda, S. Hirono, K. Yamazaki, T. Yamori, Antitumor activity of ZSTK474, a new phosphatidylinositol 3-kinase inhibitor, *J. Natl. Cancer Inst.* 98 (2006) 545–556.
- [12] E.H. Walker, M.E. Pacold, O. Perisic, L. Stephens, P.T. Hawkins, M.P. Wymann, R.L. Williams, Structural determinants of phosphoinositide 3-kinase inhibition by wortmannin, LY294002, quercetin, myricetin, and staurosporine, *Mol. Cell* 6 (2000) 909–919.
- [13] E.H. Walker, O. Perisic, C. Ried, L. Stephens, R.L. Williams, Structural insights into phosphoinositide 3-kinase catalysis and signalling, *Nature* 402 (1999) 313–320.
- [14] P. Workman, P.A. Clarke, F.I. Raynaud, R.L. van Montfort, Drugging the PI3 kinase: from chemical tools to drugs in the clinic, *Cancer Res.* 70 (2010) 2146–2157.
- [15] Z.A. Knight, B. Gonzalez, M.E. Feldman, E.R. Zunder, D.D. Goldenberg, O. Williams, R. Loewith, D. Stokoe, A. Balla, B. Toth, T. Balla, W.A. Weiss, R.L. Williams, K.M. Shokat, A pharmacological map of the PI3-K family defines a role for p110 α in insulin signaling, *Cell* 125 (2006) 733–747.
- [16] F.I. Raynaud, S. Eccles, P.A. Clarke, A. Hayes, B. Nutley, S. Alix, A. Henley, F. Di-Stefano, Z. Ahmad, S. Guillard, L.M. Bjerke, L. Kelland, M. Valenti, L. Patterson, S. Gowan, A. de Haven Brandon, M. Hayakawa, H. Kaizawa, T. Koizumi, T. Ohishi, S. Patel, N. Saghir, P. Parker, M. Waterfield, P. Workman, Pharmacologic characterization of a potent inhibitor of class I phosphatidylinositol 3-kinases, *Cancer Res.* 67 (2007) 5840–5850.
- [17] S. Bach, M. Knockaert, J. Reinhardt, O. Lozach, S. Schmitt, B. Baratte, M. Koken, S.P. Coburn, L. Tang, T. Jiang, D.C. Liang, H. Galons, J.F. Dierick, L.A. Pinna, F. Meggio, F. Totzke, C. Schächtele, A.S. Lerman, A. Carnero, Y. Wan, N. Gray, L. Meijer, Roscovitine targets, protein kinases and pyridoxal kinase, *J. Biol. Chem.* 280 (2005) 31208–31219.
- [18] APEX2. Version 2.1. Bruker AXS Inc., Madison, Wisconsin, USA.
- [19] SHELXTL. Version 5.1. Bruker AXS Inc., Madison, Wisconsin, USA.
- [20] G.M. Sheldrick. SHELX97. Program for the Refinement of Crystal Structures. University of Gottingen, Germany.
- [21] Sybyl 8.0, Tripos Associates, Inc. 1699 South Hanley Road, St. Louis, MO 63144, U.S.A.
- [22] M. Clarck, R.D. Cramer III, N. Van Opdenbosch, Validation of the general purpose Tripos 5.2 force field, *J. Comput. Chem.* 10 (1989) 982–1012.
- [23] G. Jones, P. Willet, R.C. Glen, Development and validation of a genetic algorithm for flexible docking, *J. Mol. Biol.* 267 (1997) 727–748.